ADVANCED OPTICAL MATERIALS
www.advopticalmat.de

Creation and Annihilation of Nonradiative Recombination Centers in Polycrystalline Metal Halide Perovskites by Alternating Electric Field and Light

*Ruiyun Chen, Jun Li, Alexander Dobrovolsky, Soranyel González-Carrero, Marina Gerhard, Maria E. Messing, Vladimir Chirvony, Julia Pérez-Prieto, and Ivan G. Scheblykin**

Metal halide perovskites are promising optoelectronic materials. Their electronic properties however are rather unstable which is often assigned to ion migration. Ion migration can be readily influenced by an electric field (EF). Here, the response of photoluminescence (PL) of individual $MAPbX_3$ ($MA = CH_3NH_3$, X = I, Br) sub-micrometer-sized polycrystals to EF is studied. Alternating EF with frequency higher than 10 Hz is found to reversibly quench PL. It is proposed that an alternating EF when applied together with light increases ion migration. This leads to a shift in the equilibrium between creation and annihilation of defects toward higher concentration of nonradiative recombination centers. The PL quenching is found to increase with increasing frequency of the field. This can be rationalized by the frequency dependence of the dielectric constant, leading to stronger internal fields for high modulation frequencies compared to, e.g., a constant EF with the same external amplitude. PL quenching and enhancement observed under constant EF are hypothesized to be due to a reconfiguration of already existing nonradiative recombination centers situated on grain boundaries. The control of perovskite PL by alternating EF reported here can find applications in optoelectronic devices.

1. Introduction

The past decade has seen a rapid development of solar cells based on metal halide perovskites (MHPs) benefiting from their advantages such as low-temperature processing, high absorption coefficient, long electron–hole diffusion length, and tuneable band gap.[1–4] However, the instability of MHP materials remains a major hurdle that limits the commercialization of the perovskite solar cells, particularly under operating conditions such as illumination and electrical bias. Recent literature indicates that ion migration is intrinsic to MHP, and it contributes to many effects in perovskite materials and devices such as hysteresis, photo-induced giant dielectric constants, photoluminescence (PL) enhancement, degradation, blinking and flickering, and so on.[5–15] Ion migration has also been reported to be responsible for the formation of structural defects and eventual degradation of perovskite semiconductors.[6,16–19] Defect states in MHP have been widely discussed in literature because of their direct influence on the carrier lifetime and diffusion length, which are crucial for reaching high efficiency of the MHP-based devices.[20–26] However, the defect states can also be annihilated as demonstrated, e.g., by PL enhancement by light soaking and solar cells efficiency recovery after keeping devices in dark which complicates the picture.[27,28] Although substantial efforts have been made to study ion migration under illumination and external electric field (EF),[6–8,13,16,29,30] the underlying fundamental physics concerning nonradiative recombination induced by ion migration remains elusive. A deeper insight into the ion migration effect in MHP, particularly under illumination and external bias, is imperative to solve the instability problem of perovskite-based devices.

Recently, EF poling experiments on MHP films with lateral electrodes have shown both reversible and irreversible PL quenching, which has been attributed to the formation of traps due to ion migration.[31,32] In most of the experiments, however, perovskite films or crystals were directly in contact with at least one of the electrodes.[6,30–36] This makes direct charge injection and decomposition of the material under prolonged influence of current an important factor for the PL response. Thus lack of insulation layers makes it difficult to tell apart the pure effect of

Dr. R. Chen, J. Li, Dr. A. Dobrovolsky, Dr. M. Gerhard, Prof. I. G. Scheblykin
Division of Chemical Physics and NanoLund
Lund University
P.O. Box 124, 22100 Lund, Sweden
E-mail: ivan.scheblykin@chemphys.lu.se
Dr. R. Chen
State Key Laboratory of Quantum Optics and Quantum Optics Devices
Institute of Laser Spectroscopy
Shanxi University
Taiyuan 030006, China
Dr. S. González-Carrero, Dr. V. Chirvony, Prof. J. Pérez-Prieto
Instituto de Ciencia Molecular
Universitat de Valencia
c/Catedrático J. Beltrán, 2, Paterna 46980, Spain
Prof. M. E. Messing
NanoLund and Division of Solid State Physics
Lund University
P.O. Box 118, 22100 Lund, Sweden
Dr. V. Chirvony
UMDO (Unidad de Materiales y Dispositivos Optoelectrónicos)
Instituto de Ciencia de los Materiales
Universitat de Valencia
Valencia 46071, Spain
The ORCID identification number(s) for the author(s) of this article can be found under https://doi.org/10.1002/adom.201901642.

DOI: 10.1002/adom.201901642

EF from the effect of prolonged current and mass transfer over the device.

The difference of our approach is that we want to exclude direct charge injection in order to have a better insight into the EF-induced PL response. To achieve this, we studied individual sub-micrometer MHP polycrystals in devices with well-insulated electrodes. The PL properties of two types of MHP polycrystals ($MAPbX_3$, X = Br, I) were studied under both constant EF and alternating EF. It was found that the PL of $MAPbBr_3$ shows various responses to the constant EF including PL enhancement and quenching, while for $MAPbI_3$ only PL quenching was observed under constant EF. However, the PL of both materials was found to be easily quenched by alternating EF with frequencies 10–1000 Hz. After removing the alternating EF, the PL was found to slowly recover within several minutes to the original value. We will discuss the difference between constant and alternating EF and the role of grain boundaries and light-induced ion migration for the observed effects. The ability to control PL by EF can be potentially used in optoelectronic devices.

2. PL and Scanning Electron Microscope (SEM) Image Analysis of Individual $MAPbBr_3$ Polycrystals

Figure 1a shows the typical PL image of an $MAPbBr_3$ sample prepared on an interdigitated electrode device (see the Experimental Section). The bright spots presented in this image show individual $MAPbBr_3$ polycrystals which are also visible in the corresponding SEM image (Figure 1b). The full set of individual crystals and their labeling scheme are presented in Figure S4 in the Supporting Information. Note that some small crystals were sometimes staying in long-lived off states and were not always visible on PL images, compare Figure 1a and Figure S4 in the Supporting Information, where PL images of the same region were taken at different times. The simulated distribution of EF between two electrodes under 50 V constant bias is shown in Figure 1c, demonstrating that a large EF amplitude is reached at the edges of the electrodes. Due to the device profile, most of the crystals appeared sitting at the edges of the electrodes where the EF was the strongest (up to 4×10^5 V cm^{-1}). Figure 1d shows an SEM image of the individual $MAPbBr_3$ polycrystal no. 63, which is also marked on the images in (a) and (b). SEM images of some other crystals can be found in Figure S3 in the Supporting Information.

3. PL Response of Different Individual $MAPbBr_3$ Polycrystals under 50 V Constant EF

We investigated the PL response of $MAPbBr_3$ and of $MAPbI_3$ crystals on a constant and sinusoidal EF by applying either constant or alternating bias voltage. We varied the modulation frequency from 0 Hz to 1 kHz and used the bias amplitude up to 50 and 100 V for $MAPbBr_3$ and $MAPbI_3$, respectively.

Figure 2 shows several typical responses of the PL of individual $MAPbBr_3$ polycrystals to a constant bias (50 V, EF up to 4×10^5 V cm^{-1} at the electrode edge). Data for all studied crystals are shown in Figure S5 in the Supporting Information. In this experiment, the laser was always kept on, but the EF was switched on at 10 s and switched off at 20 s. It was found that the PL of about 75% of the crystals did not show clear response to the applied constant EF. The other crystals, however, showed a very diverse and often delayed response. PL of some polycrystals was quenched when the constant bias was switched on with PL recovery after the constant bias was switched off. This is consistent with the reported effects in EF poling experiments.[31] Contrary to previous reports, we also found a significant enhancement of the PL of some crystals induced by constant EF (Figure 2c,d). Although the response can be

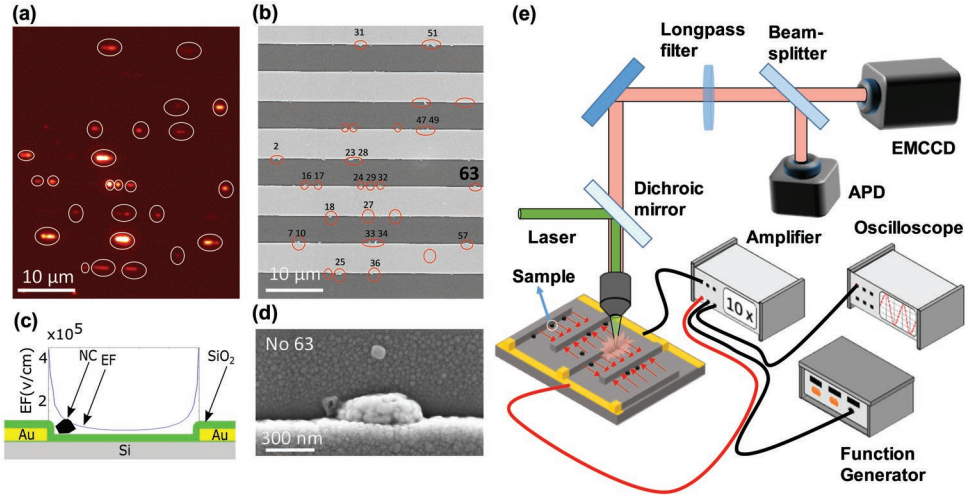

Figure 1. a) PL image of $MAPbBr_3$ nano and microcrystals dispersed on the device with interdigitated electrodes with 5 µm gap. b) SEM image of the same region of the device where electrodes and some crystals are visible, circles mark the same areas in (a) and (b), crystals are labeled by numbers. c) The scheme of the device (not in scale), thicknesses of the layers: Au—210 nm, SiO_2—140 nm. The distribution of the EF over the electrode gap is calculated for 50 V constant voltage applied between neighboring electrodes using COMSOL simulation software. Close to the electrode edge, the EF reaches 4×10^5 V cm^{-1}. d) SEM image of crystal no. 63 marked in (b). e) Overview of the experimental setup.

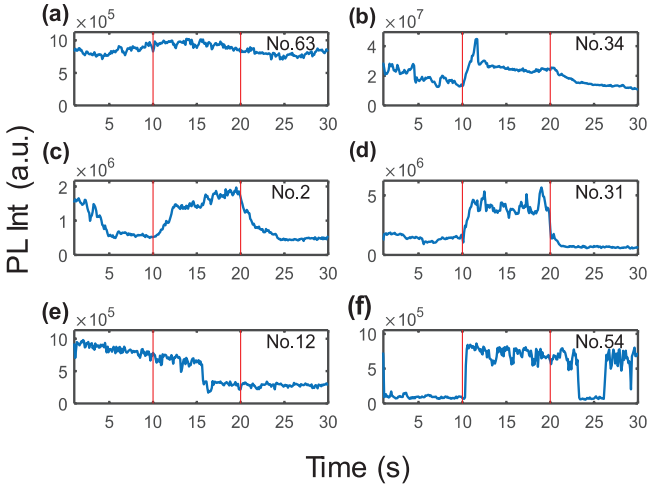

Figure 2. PL intensity traces of several individual $MAPbBr_3$ crystals demonstrating diverse response to 50 V constant bias. Times when the EF was switched on and off are marked by red vertical lines.

both fast and slow, the examples presented in Figure 2c,d show a direct correlation between the PL intensity change and the timing of the constant bias switching. More interestingly, some crystals showed a delayed response to the constant EF switching (Figure 2e,f), however, here we cannot fully exclude the influence of intrinsic PL intermittency of the polycrystal itself. We propose that the diverse response to a constant EF is related to heterogeneity of the studied crystals in terms of polycrystallinity, morphology, and initial distribution of defects as will be further discussed in more details.

4. PL Response of Different Individual $MAPbBr_3$ Polycrystals to 50 V@1 kHz Alternating EF

In contrast to the heterogenous response of individual crystals to a constant EF, a much more homogenous response to an alternating EF was observed—namely, the PL of all studied crystals

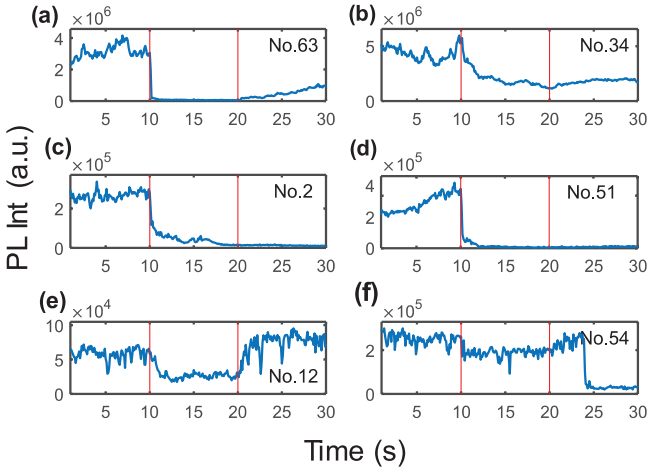

Figure 3. PL intensity traces of several $MAPbBr_3$ polycrystals showing similar responses to 50 V@1 kHz alternating bias. Times when the EF was switched on and off are marked by red vertical lines.

was quenched. **Figure 3** shows the influence of alternating EF on PL intensity traces of the same individual $MAPbBr_3$ crystals whose response to a constant EF has been shown in Figure 2. PL responses of all crystals to the alternating EF are shown in Figure S6 in the Supporting Information. These results demonstrate that the PL was quenched significantly when an alternating bias (±50 V, 1 kHz) was applied. After removing the alternating EF, the PL recovered to its original level at the time scale of minutes (not shown).

5. Bias Voltage and Frequency-Dependent PL Quenching of Individual $MAPbBr_3$ Polycrystals under Alternating EF

To assess the effect of the EF amplitude, the bias voltage of alternating EF was swept from ±10 to ±50 V with the fixed frequency of 1 kHz (**Figure 4**a). Here, the background level was subtracted first from the PL signal and then the intensity was divided by the PL intensity averaged over the first 10 s (before applying the EF). It can be seen that the PL of an individual $MAPbBr_3$ was not quenched under ±10 V alternating EF. However, when the alternating EF amplitude was increased to ±20 V, the quenching became pronounced. When the EF amplitude was increased further, the PL was completely quenched to the background level.

Figure 4b shows the normalized PL of another $MAPbBr_3$ crystal (crystal no. 63) under alternating EF with ±50 V bias amplitude but the frequency was swept from 1 Hz to 1 kHz. It can be seen that the PL shows a very little response to the alternating EF under 1 Hz. However, increasing the frequency leads to a more pronounced PL quenching. At 1 kHz and 50 V amplitude, the PL of the $MAPbBr_3$ crystals was quenched to the background level. Moreover, the recovery process was much slower for 1 kHz in comparison to the recovery after applying an alternating EF of lower frequencies.

The PL spectrum of crystal no. 63 was measured before and during the application of alternating bias (±50 V, 1 kHz), as shown in Figure 4c. While PL was quenched, no spectral shift was observed. We also compared the PL decay of the same individual polycrystal before and during alternating bias (±50 V, 1 kHz). Figure 4d shows that the PL decay kinetic without EF is close to mono-exponential. However, under the alternating bias the PL decays much faster nonexponentially. Upon removal of the alternating bias, the decay recovers completely to the initial shape (yellow line) accompanied by recovery of the PL intensity.

6. The Role of Light Illumination and Alternating EF in PL Quenching and Recovery of $MAPbBr_3$ Polycrystals

Here, two questions arise when we consider the role of illumination and EF in PL quenching and recovery. First, is alternating EF the only responsible for PL quenching? Is light illumination also important? Second, does light illumination play a role in the recovery process of PL after removing EF? A

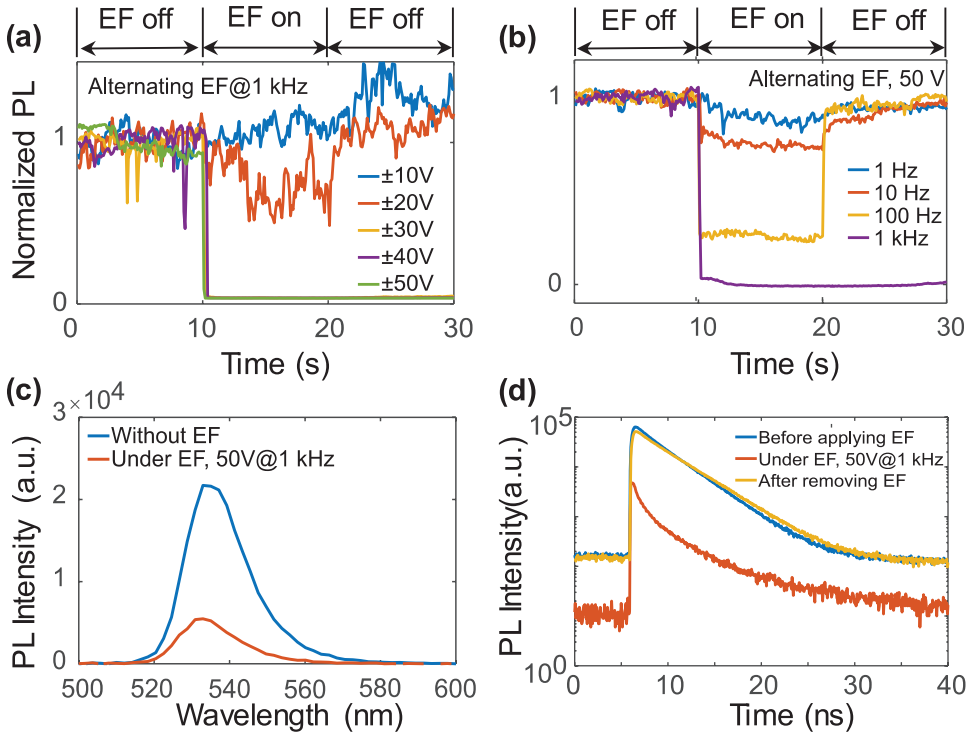

Figure 4. a) Normalized PL intensity traces of an individual $MAPbBr_3$ polycrystal under 1 kHz alternating EF with different bias amplitude. b) Normalized PL intensity traces of another individual $MAPbBr_3$ crystal (no. 63) under ±50 V alternating bias with different frequency. The sample was irradiated by the laser over the whole measurement. c) PL spectra of the individual $MAPbBr_3$ crystal (no. 63) without and with ±50 V@1 kHz alternating bias. d) PL decay curves of the individual $MAPbBr_3$ crystal (no. 63) with and without ±50 V@1 kHz alternating bias.

series of experiments on the individual $MAPbBr_3$ polycrystal no. 63 to answer these questions will be presented below.

For each experiment, we used different time sequence in which both the bias and the laser were switched on and off in various patterns (see **Figure 5**). At first, we checked the response of the PL on switching on and off the laser only. With our time resolution, the response was instantaneous (Figure 5a, gray coloring shows the dark condition). Then we monitored the response of PL on switching on and off alternating EF under constant laser illumination. While the PL quenching was fast, the PL recovery was much slower at the time scale of minutes (Figure 5b). In the next experiment, we applied the same alternating bias during the time the laser was switched off (Figure 5c). Just a second after the bias was removed, we photoexcited the crystal again and followed the evolution of the PL intensity. In this case, PL recovery to its original value was substantially faster than in case b when the EF and the laser acted together. Therefore, simultaneous application of light and alternating EF induces stronger and more enduring changes in the material compared to an alternating EF alone.

In the last test shown in Figure 5d, we checked how fast the sample recovers without illumination after switching the bias off. Essentially the experiment was the same as in case b, but after removing the bias we also removed the laser illumination for 10 s. After this dark period, the PL recovered more slowly than in case b (see also Figure S7, Supporting Information). It shows that laser illumination does not only lead to a larger change in the material when applied together with EF, but also helps the material to recover to its original state.

7. Bias Voltage and Frequency-Dependent PL Quenching of $MAPbI_3$ Polycrystals under Alternating EF

We carried out the same experiments with $MAPbI_3$ polycrystals. The PL and SEM images of the sample are shown in Figure S8 in the Supporting Information. The influence of the bias voltage on the PL of the $MAPbI_3$ polycrystal (no. 28 in Figure S10, Supporting Information) is shown in **Figure 6**a, in which the alternating bias voltage was swept from ±10 to ±100 V with fixed modulation frequency of 1 kHz. Similar to $MAPbBr_3$, higher bias voltage and higher frequency gave stronger PL quenching (Figure 6b). Likewise, no spectral shift upon EF-induced quenching was observed (Figure 6c). The PL decay of the $MAPbI_3$ polycrystal before and during alternating EF (±50 V@1 kHz) is shown in Figure 6d where only a quite small change of PL lifetime upon EF-induced quenching can be seen. The PL recovery process in $MAPbI_3$ (Figure S9, Supporting Information) appears to be faster than that in the $MAPbBr_3$ sample, compare with Figure 5. Another significant difference is that the constant EF was found to cause only a weak PL quenching in some of the studied $MAPbI_3$ crystals, but no PL enhancement was observed contrary to the $MAbBr_3$ sample (see Figure S11, Supporting Information).

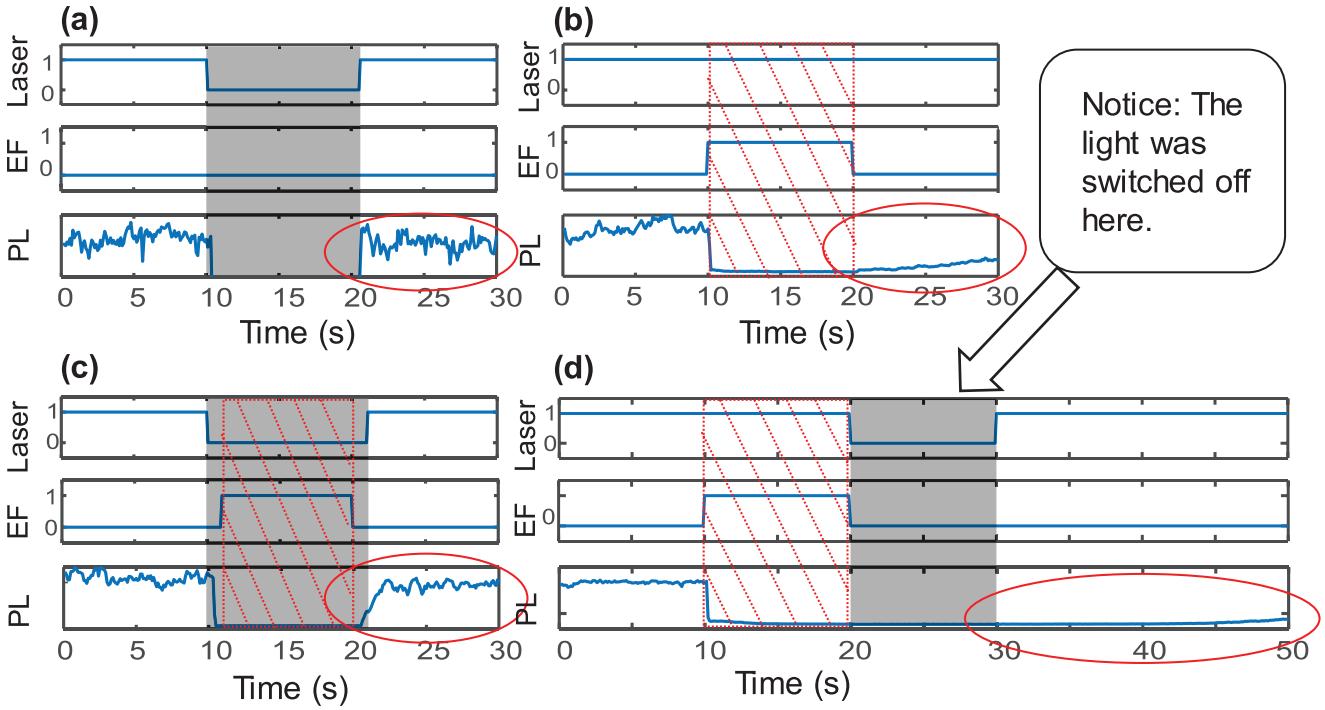

Figure 5. PL intensity transients of the individual $MAPbBr_3$ polycrystal (no. 63) under light irradiation and alternating bias (±50 V@1 kHz) applied in different combinations. a) The laser was switched on and off without bias (dark period is shown by gray coloring). b) The laser was always on while the EF was switched on and then off (red hatching). c) EF was applied during the period when the laser was switched off. d) The same experiment as in (b) but the laser was switched off for 10 s at the same time with switching off the EF. Compare the PL recovery kinetics in all graphs, marked by red ellipses.

8. Possible Mechanisms of PL Response of $MAPbX_3$ Polycrystals to Constant and Alternating EF

Under photoexcitation only a minor part of the absorbed energy is emitted as PL because the PL quantum yield is quite low. Thus, most of the photo-generated charges recombine nonradiatively generating not only heat but also chemical/structural modifications of the material. Generally speaking, nonradiative recombination occurs via charge trapping by defect states lying close to the middle of the bandgap, by nonradiative centers of a complex internal organization (like, e.g., donor–acceptor pairs) and by surface states.[37–39] For $MAPbI_3$, the most widely discussed native point defects are iodine vacancies (V_I) and anti-site occupations (Pb_I and I_{MA}).[20–23] Frenkel defects (the simplest defect complex consisting of an interstitial defect and a vacancy created by the same atom) have also been discussed as possible effective nonradiative centers.[27]

There are many factors at the preparation stage which can induce defects in MHP.[40,41] However, when the sample is already prepared, ion migration is probably one of the most important phenomenon responsible for further sample evolution and its eventual degradation.[17,18,42] The dominant species for ion migration are most likely the halogen ions (e.g., I^- in $MAPbI_3$), however MA^+ and others can also migrate but with higher activation energy.[11,13,30,43] It is known that light illumination can induce and enhance ion migration in MHP materials by yet not fully understood mechanisms.[10,27,29] Both light-induced PL enhancement and PL degradation have been discussed in relation to ion migration which can assist annihilation and creation of defects.[44–46]

When an MHP material is placed in an external EF, both free charges and ions are able to drift along the field direction.[33,43] As a first approximation, the averaged EF inside the material is lower than that outside by an effective dielectric constant ε. MHP and in particular $MAPbI_3$ and $MAPbBr_3$ possess an apparent giant ε reaching 1000 or more for a static EF. For an AC EF, ε goes down by one to two orders of magnitude with increasing of the frequency to 1 kHz.[9] Literature discusses many reasons for such high value of ε and its frequency dependence.[9,14,47,48] Local inhomogeneity in terms of capacity and conductivity as well as ion migration is considered to be an importnant factor leading to the complex dielectric response of MHPs.[9,14] Although there is no comprehensive picture yet, it is clear that a constant equilibrated EF inside the material should be much lower than an alternating EF at frequencies 0.1–1 kHz due to the difference in the apparent dielectric constant.

Because the internal static EF is weak, the effect of the constant EF to $MAPbX_3$ crystals, if it exists at all, must be highly dependent on the initial condition of the crystals. In other words, we propose that a static EF is able to change the status of already existing nonradiative centers, but it is too week to create new ones. For example, let us look at the results for $MAPbBr_3$. As can be found in the SEM images, different $MAPbBr_3$ polycrystals possess very different morphologies. In some of them we see many grain boundaries (Figure 1d and Figure S3, Supporting Information). The grain boundaries separate highly conductive crystals and charge carriers (ions, electrons, holes)

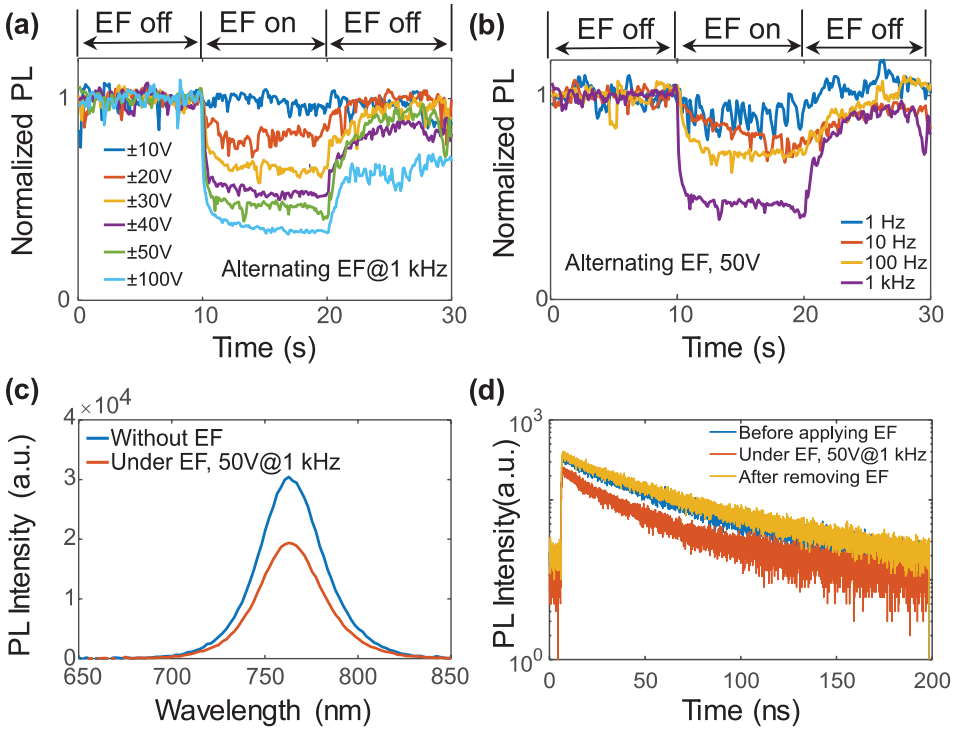

Figure 6. PL intensity transients, spectra, and decay kinetics for individual $MAPbI_3$ crystal no. 28 under influence of AC EF. a) The PL intensity transients under influence of 1 kHz AC EF with different bias voltage applied at 10 s and removed at 20 s. b) The PL intensity traces under influence of ±50 V AC EF with different frequency applied at 10 s and removed at 20 s. The laser remained on during the whole measurements in (a) and (b). c) PL spectra before and during application of AC EF (±50 V@1 kHz). d) PL decay kinetics before, during, and after applying AC EF (±50 V@1 kHz).

may accumulate at the interfaces or their pre-existing configurations may change upon application of EF. This means that the conditions at the surface of the crystallites inside the polycrystalline agglomerate (in terms of locations of ions, and their complexes) can change under EF leading to changing of the surface recombination rate and, as a consequence, PL quantum yield. Due to different and individual crystallization conditions, the individual "history" of each crystal in terms of the number, location, and shape of the grain boundaries differs enormously from crystal to crystal. That is why we can find very diverse responses of $MAPbBr_3$ polycrystals to constant EF (Figure 2). Since reconfiguration of the surface charges may take time and may have a high potential barrier, the response can be delayed as shown in Figure 2 for some crystals. Ideas along these lines have been used to speculate about the nature of EF-dependent luminescence blinking of perovskite quantum dots and individual molecules of conjugated polymers.[49,50]

In contrast, when the alternating EF with high frequency was applied to the samples of both $MAPbI_3$ and $MAPbBr_3$, the internal field was about one order of magnitude higher than for the constant EF condition. Strong EF induces separation of electron and holes and also pulls apart ions of the opposite sign. We hypothesize that this field is strong enough to generate new nonradiative recombination centers by inducing local ion migration[36] in the material illuminated by light. That is why, we always observed PL quenching under the alternating EF conditions. We found that the effect of EF gets much stronger in terms of long-lasting change of the sample PL when light illumination is applied at the same time (compare the recovery time after switching off EF in Figure 5a,b, and in Figure S9a,b, Supporting Information).

Naturally, ion migration induced by the laser illumination must be further promoted by the EF, leading to the formation of structural defects and nonradiative recombination centers.[8,13,27,29] Neither our data nor the literature allows for comprehensive discussion of the nature of these nonradiative centers much beyond speculation. When the external alternating EF was removed from the perovskite polycrystals, the PL showed a slow recovery. The recovery is slow simply because it is driven by temperature and may be light, while the formation of quenchers is also driven by EF. When the crystal structure has recovered, the PL intensity reaches the original level. Note that PL recovery was much slower without the assistance of light illumination, as can be found in Figure S7 in the Supporting Information by comparison with Figure 5d. We propose that annihilation of the structural defects in the dark is so slow because ion migration without light is slow.[8,29]

Our experimental results allow us to propose a simple qualitative model based on chemical equilibrium. Let us assume that we have two states of the semiconductor called Bright and Dark. In the Bright state, the concentration of nonradiative centers is small and PL intensity is high, while in the Dark state the concentration of nonradiative centers is large and PL is quenched. These two states are in equilibrium due to continuous formation and annihilation of nonradiative centers with rates k and k', respectively, which become larger upon light illumination due to light assistant ion migration. Obviously, an alternating EF promotes the Dark state with respect to the Bright state,

or, in other words, it shifts the chemical equilibrium toward a higher concentration of nonradiative centers. The role of light illumination is then to accelerate the process, i.e., to shorten the time needed to reach the equilibrium between the defect formation and annihilation. Formally, we can express this idea by using EF-dependent equilibrium constant K in the following reaction

$$\text{Bright} \underset{k'(\text{light})}{\overset{k(\text{light})}{\rightleftharpoons}} \text{Dark}, \qquad K(\text{EF}) = \frac{[\text{Bright}]}{[\text{Dark}]} \tag{1}$$

9. Conclusion

We studied the effect of EF on the PL of sub-micrometer polycrystals of $MAPbX_3$(X = Br, I) perovskite. Unlike most published experiments, we employed devices where insulation prevented direct charge injection to the material from electrodes. It was found that a constant EF shows very individual effects on PL of $MAPbBr_3$ polycrystals ranging from PL quenching to PL enhancement and from an immediate to a delayed response. A substantial part of the studied crystals showed no response to constant EF at all. This is contrary to alternating EF, which was found to reversibly quench the PL of all studied crystals for both perovskite materials. We propose that alternating EF has such a clear effect first of all due to the orders of magnitude higher EF inside the crystals in comparison to the constant EF due to a lower dielectric constant for alternating EF (1 kHz) in comparison with the static conditions. This alternating EF is able to create nonradiative recombination centers by promoting ion migration. The constant field, although much weaker, acts for a long time uni-directionally, which eventually can change the status of already existing nonradiative centers and states at the surfaces and grain boundaries. This can lead to either changes of PL (quenching or enhancement) depending on the initial conditions in the crystal. In all experiments, the rate of creation and annihilation of the PL quenching centers showed clear dependence on the light illumination conditions as expected for an ion-migration-induced process. The whole observations fit the qualitative picture where the external EF determines the balance between the radiative and nonradiative recombination (equilibrium conditions) while light illumination influences the speed the equilibrium is reached. Besides fundamental interest, our results can be useful in application of MHP as optoelectronic switches including neuromorphic optoelectronics where responses with memory/delay can be of an advantage.[51]

10. Experimental Section

A device consisting of gold interdigitated electrodes with 5 µm gaps was fabricated on thermally oxidized silicon wafers using standard photolithographic techniques. The contact area of the device was covered by a 140 nm thick SiO_2 layer to isolate the perovskite crystals from the electrodes. The colloidal solution of "naked" $MAPbBr_3$ nanocrystals without surfactant was prepared according to the published recipe.[52] It was diluted with ethyl acetate and drop-cast on the device. $MAPbI_3$ sample was prepared via the one-step process using *gamma*-Butyrolactone as the solvent. The diluted precursor solution was drop-cast on the device, followed by 20 min thermal annealing at 80 °C (see the Supporting Information for detailed information). The device containing perovskite polycrystals was mounted on the sample stage of a home-built wide-field epi-fluorescence microscope based on an Olympus IX71 frame, as shown in Figure 1e and Figure S1 in the Supporting Information. The samples were excited by an Argon-ion laser (514 nm, CW) through a 40 × objective (Olympus LUCPlanFL, NA = 0.6) resulting in an excitation power density of 1.8 W cm^{-2} for $MAPbBr_3$ and 0.27 W cm^{-2} for $MAPbI_3$ polycrystals, respectively. An EMCCD camera (ProEM 512B, Princeton Instruments) was used to record PL images and PL spectra of individual crystals. A constant or sine-wave alternating bias voltage was generated by a function generator as shown in Figure S2 in the Supporting Information. In order to obtain PL lifetime of the perovskite polycrystals, a pulsed 485 nm diode laser (10 MHz, 1.55 W cm^{-2} for $MAPbBr_3$ and 5 MHz, 0.82 W cm^{-2} for $MAPbI_3$) was used for excitation. The PL was then detected by a single photon counting system (PicoHarp, time resolution ≈100 ps). All measurements were carried out in ambient air at room temperature.

Supporting Information

Supporting Information is available from the Wiley Online Library or from the author.

Acknowledgements

R.C. and J.L. contributed equally to this work. This work was supported by the Swedish Research Council (2016-04433) and Swedish Research Council collaborative grant with China (2017-00748). J.L. thanks China Scholarship Council (CSC No. 201608530162) for a Ph.D. scholarship. A.D. acknowledges the Carl Trygger Foundation for a postdoctoral scholarship. R.C. thanks the Shanxi Scholarship Council of China (no. 20171672). M.G. acknowledges the Wenner-Gren foundation for a postdoctoral fellowship (UPD2017-0223). Part of the work has been performed within Lund NanoLab with financial support from NanoLund and Myfab. The authors also thank MINECO (CTQ2017-82711-P, partially co-financed with FEDER funds; Maria de Maeztu: MDM-2015-0538; and FPI grant to S.G.C.).

Conflict of Interest

The authors declare no conflict of interest.

Keywords

electric field, ion migration, metal halide perovskites, nonradiative recombination, photoluminescence

Received: September 29, 2019
Published online: December 9, 2019

[1] J. You, Z. Hong, Y. Yang, Q. Chen, M. Cai, T.-B. Song, C.-C. Chen, S. Lu, Y. Liu, H. Zhou, Y. Yang, *ACS Nano* **2014**, *8*, 1674.
[2] L. Dou, Y. Yang, J. You, Z. Hong, W.-H. Chang, G. Li, Y. Yang, *Nat. Commun.* **2014**, *5*, 5404.
[3] F. Zhang, S. Huang, P. Wang, X. Chen, S. Zhao, Y. Dong, H. Zhong, *Chem. Mater.* **2017**, *29*, 3793.
[4] S. D. Stranks, G. E. Eperon, G. Grancini, C. Menelaou, M. J. P. Alcocer, T. Leijtens, L. M. Herz, A. Petrozza, H. J. Snaith, *Science* **2013**, *342*, 341.

[5] Y. Kimura, I. Karimata, Y. Kobori, T. Tachikawa, *ChemNanoMat* **2019**, *5*, 340.
[6] Y. Yuan, J. Huang, *Acc. Chem. Res.* **2016**, *49*, 286.
[7] S. G. Motti, D. Meggiolaro, A. J. Barker, E. Mosconi, C. A. R. Perini, J. M. Ball, M. Gandini, M. Kim, F. De Angelis, A. Petrozza, *Nat. Photonics* **2019**, *13*, 532.
[8] Y. C. Zhao, W. K. Zhou, X. Zhou, K. H. Liu, D. P. Yu, Q. Zhao, *Light: Sci. Appl.* **2017**, *6*, e16243.
[9] E. J. Juarez-Perez, R. S. Sanchez, L. Badia, G. Garcia-Belmonte, Y. S. Kang, I. Mora-Sero, J. Bisquert, *J. Phys. Chem. Lett.* **2014**, *5*, 2390.
[10] M. Anaya, J. F. Galisteo-López, M. E. Calvo, J. P. Espinós, H. Míguez, *J. Phys. Chem. Lett.* **2018**, *9*, 3891.
[11] C. Li, A. Guerrero, Y. Zhong, A. Gräser, C. A. M. Luna, J. Köhler, J. Bisquert, R. Hildner, S. Huettner, *Small* **2017**, *13*, 1701711.
[12] J. M. Frost, A. Walsh, *Acc. Chem. Res.* **2016**, *49*, 528.
[13] C. Eames, J. M. Frost, P. R. F. Barnes, B. C. O'Regan, A. Walsh, M. S. Islam, *Nat. Commun.* **2015**, *6*, 2.
[14] I. Anusca, S. Balčiūnas, P. Gemeiner, Š. Svirskas, M. Sanlialp, G. Lackner, C. Fettkenhauer, J. Belovickis, V. Samulionis, M. Ivanov, B. Dkhil, J. Banys, V. V. Shvartsman, D. C. Lupascu, *Adv. Energy Mater.* **2017**, *7*, 1700600.
[15] M. Gerhard, B. Louis, R. Camacho, A. Merdasa, J. Li, A. Kiligaridis, A. Dobrovolsky, J. Hofkens, I. G. Scheblykin, *Nat. Commun.* **2019**, *10*, 1698.
[16] S. Bae, S. Kim, S. W. Lee, K. J. Cho, S. Park, S. Lee, Y. Kang, H. S. Lee, D. Kim, *J. Phys. Chem. Lett.* **2016**, *7*, 3091.
[17] H. Yuan, E. Debroye, K. Janssen, H. Naiki, C. Steuwe, G. Lu, M. Moris, E. Orgiu, H. Uji-I, F. De Schryver, P. Samorì, J. Hofkens, M. Roeffaers, *J. Phys. Chem. Lett.* **2016**, *7*, 561.
[18] C. Besleaga, L. E. Abramiuc, V. Stancu, A. G. Tomulescu, M. Sima, L. Trinca, N. Plugaru, L. Pintilie, G. A. Nemnes, M. Iliescu, H. G. Svavarsson, A. Manolescu, I. Pintilie, *J. Phys. Chem. Lett.* **2016**, *7*, 5168.
[19] C. Li, S. Tscheuschner, F. Paulus, P. E. Hopkinson, J. Kießling, A. Köhler, Y. Vaynzof, S. Huettner, *Adv. Mater.* **2016**, *28*, 2446.
[20] J. M. Ball, A. Petrozza, *Nat. Energy* **2016**, *1*, 16149.
[21] J. Kim, S. H. Lee, J. H. Lee, K. H. Hong, *J. Phys. Chem. Lett.* **2014**, *5*, 1312.
[22] W. J. Yin, T. Shi, Y. Yan, *Appl. Phys. Lett.* **2014**, *104*, 063903.
[23] M. L. Agiorgousis, Y. Y. Sun, H. Zeng, S. Zhang, *J. Am. Chem. Soc.* **2014**, *136*, 14570.
[24] A. Walsh, D. O. Scanlon, S. Chen, X. G. Gong, S. H. Wei, *Angew. Chem., Int. Ed.* **2015**, *54*, 1791.
[25] A. Buin, P. Pietsch, J. Xu, O. Voznyy, A. H. Ip, R. Comin, E. H. Sargent, *Nano Lett.* **2014**, *14*, 6281.
[26] A. Buin, R. Comin, J. Xu, A. H. Ip, E. H. Sargent, *Chem. Mater.* **2015**, *27*, 4405.
[27] E. Mosconi, D. Meggiolaro, H. J. Snaith, S. D. Stranks, F. De Angelis, *Energy Environ. Sci.* **2016**, *9*, 3180.
[28] W. Nie, J.-C. Blancon, A. J. Neukirch, K. Appavoo, H. Tsai, M. Chhowalla, M. A. Alam, M. Y. Sfeir, C. Katan, J. Even, S. Tretiak, J. J. Crochet, G. Gupta, A. D. Mohite, *Nat. Commun.* **2016**, *7*, 11574.
[29] D. W. DeQuilettes, W. Zhang, V. M. Burlakov, D. J. Graham, T. Leijtens, A. Osherov, V. Bulović, H. J. Snaith, D. S. Ginger, S. D. Stranks, *Nat. Commun.* **2016**, *7*, 11683.
[30] Y. Yuan, Q. Wang, Y. Shao, H. Lu, T. Li, A. Gruverman, J. Huang, *Adv. Energy Mater.* **2016**, *6*, 1501803.
[31] X. Deng, X. Wen, C. F. J. Lau, T. Young, J. Yun, M. A. Green, S. Huang, A. W. Y. Ho-Baillie, *J. Mater. Chem. C* **2016**, *4*, 9060.
[32] C. Li, A. Guerrero, S. Huettner, J. Bisquert, *Nat. Commun.* **2018**, *9*, 5113.
[33] X. Hu, X. Wang, P. Fan, Y. Li, X. Zhang, Q. Liu, W. Zheng, G. Xu, X. Wang, X. Zhu, A. Pan, *Nano Lett.* **2018**, *18*, 3024.
[34] S. Y. Luchkin, A. F. Akbulatov, L. A. Frolova, M. P. Griffin, A. Dolocan, R. Gearba, D. A. V. Bout, P. A. Troshin, K. J. Stevenson, *ACS Appl. Mater. Interfaces* **2017**, *9*, 33478.
[35] W. Mao, J. Zheng, Y. Zhang, A. S. R. Chesman, Q. Ou, J. Hicks, F. Li, Z. Wang, B. Graystone, T. D. M. Bell, M. U. Rothmann, N. W. Duffy, L. Spiccia, Y. B. Cheng, Q. Bao, U. Bach, *Angew. Chem., Int. Ed.* **2017**, *56*, 12486.
[36] B. Chen, T. Li, Q. Dong, E. Mosconi, J. Song, Z. Chen, Y. Deng, Y. Liu, S. Ducharme, A. Gruverman, F. De Angelis, J. Huang, *Nat. Mater.* **2018**, *17*, 1020.
[37] A. Merdasa, Y. Tian, R. Camacho, A. Dobrovolsky, E. Debroye, E. L. Unger, J. Hofkens, V. Sundström, I. G. Scheblykin, *ACS Nano* **2017**, *11*, 5391.
[38] Y. Zhao, A. M. Nardes, K. Zhu, *J. Phys. Chem. Lett.* **2014**, *5*, 490.
[39] Y. Tian, A. Merdasa, M. Peter, M. Abdellah, K. Zheng, C. S. Ponseca Jr., T. Pullerits, A. Yartsev, V. Sundstrom, I. G. Scheblykin, *Nano Lett.* **2015**, *15*, 1603.
[40] C. C. Vidyasagar, B. M. Muñoz Flores, V. M. Jiménez Pérez, *Nano-Micro Lett.* **2018**, *10*, 68.
[41] P. Fassl, V. Lami, A. Bausch, Z. Wang, M. T. Klug, H. J. Snaith, Y. Vaynzof, *Energy Environ. Sci.* **2018**, *11*, 3380.
[42] S. Kim, S. Bae, S. W. Lee, K. Cho, K. D. Lee, H. Kim, S. Park, G. Kwon, S. W. Ahn, H. M. Lee, Y. Kang, H. S. Lee, D. Kim, *Sci. Rep.* **2017**, *7*, 1.
[43] S. T. Birkhold, J. T. Precht, H. Liu, R. Giridharagopal, G. E. Eperon, L. Schmidt-Mende, X. Li, D. S. Ginger, *ACS Energy Lett.* **2018**, *3*, 1279.
[44] Y. Tian, A. Merdasa, E. Unger, M. Abdellah, K. Zheng, S. Mckibbin, A. Mikkelsen, T. Pullerits, A. Yartsev, V. Sundström, I. G. Scheblykin, *J. Phys. Chem. Lett.* **2015**, *6*, 4171.
[45] X. Hu, S. Wan, Y. Tian, D. Hong, Y. Zhou, D. Xie, *ACS Photonics* **2018**, *5*, 2034.
[46] P. Fassl, Y. Zakharko, L. M. Falk, K. P. Goetz, F. Paulus, A. D. Taylor, J. Zaumseil, Y. Vaynzof, *J. Mater. Chem. C* **2019**, *7*, 5285.
[47] J. Huang, Y. Yuan, Y. Shao, Y. Yan, *Nat. Rev. Mater.* **2017**, *2*, 17042.
[48] Q. Lin, A. Armin, R. C. R. Nagiri, P. L. Burn, P. Meredith, *Nat. Photonics* **2015**, *9*, 106.
[49] D. Kumar Sharma, S. Hirata, V. Biju, M. Vacha, *ACS Nano* **2019**, *13*, 624.
[50] P. R. Hania, I. G. Scheblykin, *Chem. Phys. Lett.* **2005**, *414*, 127.
[51] W. Xu, H. Cho, Y.-H. Kim, Y.-T. Kim, C. Wolf, C.-G. Park, T.-W. Lee, *Adv. Mater.* **2016**, *28*, 5916.
[52] S. Gonzalez-Carrero, L. C. Schmidt, I. Rosa-Pardo, L. Martínez-Sarti, M. Sessolo, R. E. Galian, J. Pérez-Prieto, *ACS Omega* **2018**, *3*, 1298.